Proceedings of the 12th Workshop on Quantum Chaos and Localisation Phenomena (CHAOS 25)

Many-Particle Quantum Chaos Beyond the Ehrenfest "Number"

B. Gutkin[a] and V.A. Osipov[b,c,*]

[a]*School of Mathematical Sciences, Holon Institute of Technology, Holon 5810201, Israel*
[b]*Institute for Advanced Study in Mathematics, Harbin Institute of Technology, 92 West Da Zhi Street, Harbin 150001, China*
[c]*Suzhou Research Institute, Harbin Institute of Technology, 500 South Guandu Road, Suzhou 215104, China*

Doi: 10.12693/APhysPolA.148.S17 *e-mail: Vladimir.Al.Osipov@gmail.com

The theory of quantum chaos demonstrates the effectiveness of semiclassical methods based on periodic-orbit correlations for calculating spectral correlations in single-particle systems. However, extending this approach to the many-particle chaotic models is non-trivial. The development of a dedicated theory in the thermodynamic-semiclassical limit, where both the number of particles and $1/\hbar$ tend to infinity, is required. In this paper, we address the above problem for a chain of cat maps with local nearest-neighbor interaction. We study the correlation mechanism between classical periodic orbits, which becomes relevant in the thermodynamic-semiclassical limit. Our findings are supported by exact results and by numerical evidence obtained for the coupled cat map model.

topics: many-body quantum chaos, periodic orbits, dual-unitary systems, coupled cat maps

1. Introduction

The backbone of the semiclassical theory of spectral correlations in chaotic systems is the Gutzwiller trace formula [1, 2]. It allows us to represent the nontrivial oscillatory part of the spectral density $\rho_{\rm osc}(E)$ as a sum over a set of unstable classical periodic orbits (POs),

$$\rho_{\rm osc}(E) \sim \frac{1}{\pi\hbar}\,{\rm Re}\left(\sum_{\gamma\in{\rm PO}} A_\gamma\,{\rm e}^{{\rm i}\,S_\gamma(E)/\hbar}\right). \tag{1}$$

Quite remarkably, the trace formula involves only classical quantities, i.e., the classical action $S_\gamma(E)$ calculated along the periodic orbit γ at a given energy E and the stability factor A_γ, which also includes the Maslov phases. In 1985, Berry [3] demonstrated the potential analytical power of this approach by calculating the "diagonal" contribution $\gamma=\gamma'$ to the spectral form factor

$$K(\tau) = \int\limits_{-\infty}^{\infty}\frac{2\pi\hbar\ {\rm d}\omega}{T_H}\ \left\langle\rho_{\rm osc}\left(E+\frac{\omega}{2}\right)\rho_{\rm osc}\left(E-\frac{\omega}{2}\right)\right\rangle_E {\rm e}^{\frac{\rm i}{\hbar}\omega\tau T_H}$$
$$\approx \frac{1}{T_H^2}\left\langle\sum_{\gamma,\gamma'} A_\gamma A^*_{\gamma'}\,{\rm e}^{{\rm i}\,\frac{S_\gamma(E)-S_{\gamma'}(E)}{\hbar}}\,\delta\big(\tau-\frac{T_\gamma-T_{\gamma'}}{2T_H}\big)\right\rangle_E, \tag{2}$$

where $T_H\propto\hbar^{1-d}$ is the Heisenberg time in the d-dimensional system, and T_γ is the orbit period. To the leading order in τ, the result coincides with the random-matrix theory (RMT) prediction of the spectral form factor $K_\beta(\tau)$ for the symmetry classes $\beta=1,2,4$, thus validating the Bohigas–Giannoni–Schmit conjecture [4, 5] on the spectral universality of chaotic systems. The missing cross-terms $\gamma\neq\gamma'$ were taken into account by Sieber and Richter in [6, 7], who demonstrated that in chaotic Hamiltonian systems the non-trivial contributions to $K(\tau)$ are given by partner periodic orbits (PPOs). In configuration space, PPOs follow almost the same paths, while the succession order in time is different. The switching of order occurs in certain regions, referred to as encounters, where PPO comes close to itself (see Fig. 1a). In encounters, the action difference accumulates its non-zero value. To reach the scales $S_\gamma - S_{\gamma'}\sim\hbar$ — required for essential correlations — the encounter duration should be of the same order as the Ehrenfest time, $\tau_E\propto\log(1/\hbar)$. Accounting for PPOs with multiple encounters culminated in the derivation of a complete, universal result for spectral correlations in chaotic Hamiltonian systems [8, 9].

The scope of the PPO approach is largely restricted to systems composed of a small number (N) of particles in the limit $\hbar\to 0$. Furthermore, for the Bose–Hubbard model with L sites, it has been

shown that the "opposite thermodynamic limit", where $N \to \infty$, while the single-particle Hilbert space effective dimension $L = \hbar^{-1}$ is fixed, is accessible through the effective semiclassical theory [10]. To this end, a natural question about the more general limit in which both N and $\hbar^{-1}$ grow simultaneously has been raised. And more specifically, is the standard semiclassical theory of spectral correlations applicable in this regime? Does the universality persist, and on what time and energy scales?

At first glance, it might seem that a growing N can be interpreted just as an increase in the effective number of degrees of freedom and should not essentially affect the semiclassical theory. In fact, the motion of N particles in d-dimensional space can always be thought of as a single particle trajectory in $(N\,d)$-dimensional space. Thus, the standard correlation mechanism between POs carries over straightforwardly to the systems of N particles. However, a PO encounter within this framework would mean that at some instant in time, all N particles simultaneously approach, on a scale of $\hbar$, their previous positions. In the present paper, we demonstrate that this picture, although correct for finite N, must be fundamentally revised for systems consisting of a large number of particles. Within the model-based approach, we show that for a chaotic N-particle system, there exist PPOs with an essentially different mechanism of correlations. In particular, encounters of such trajectories do not necessarily involve all particles. Furthermore, we show that their contribution to the semiclassical theory becomes dominant when N exceeds some scale $n_E \sim \log(1/\hbar)$, which plays a role similar to the Ehrenfest time τ_E, but for the number of particles.

2. The model

Rather than considering Hamiltonian systems with continuous time dynamics, in this paper we consider a chain of N linearly coupled Arnold's cat maps [11–15]. This model was first introduced in [16] and later studied in [17–19]. It possesses two crucial properties, i.e., locality of interactions and fully chaotic dynamics. More precisely, the map

$$\Phi_N : \ (\boldsymbol{q}_t, \boldsymbol{p}_t) \to (\boldsymbol{q}_{t+1} + \boldsymbol{m}^q_{t+1}, \boldsymbol{p}_{t+1} + \boldsymbol{m}^p_{t+1}) \quad (3)$$

acts on the vectors $\boldsymbol{q}_t = \{q_{n,t}\}_{n=1}^N$, $\boldsymbol{p}_t = \{p_{n,t}\}_{n=1}^N$, where $q_{n,t}, p_{n,t} \in [0,1]$ are the coordinate and momentum of the n-th particle at time $t \in \mathbb{Z}$, respectively. The integer entries vectors $\boldsymbol{m}^q_t = \{m^q_{n,t}\}_{n=1}^N$, $\boldsymbol{m}^p_t = \{m^p_{n,t}\}_{n=1}^N$ are composed of the winding numbers along the q and p directions, ensuring that $\boldsymbol{q}_t, \boldsymbol{p}_t$ are confined to the unit $2N$-torus $\mathbb{T}^{2N}$. The generating function of the map Φ_N (details in Appendix) for the model of coupled particles is split into two parts $S(\boldsymbol{q}_t, \boldsymbol{q}_{t+1}) = S_0(\boldsymbol{q}_t, \boldsymbol{q}_{t+1}) + S_{\rm int}(\boldsymbol{q}_t)$. The first term corresponds to N uncoupled cat maps subjected to some external periodic potential ($\mathcal{V}(q+1) = \mathcal{V}(q)$),

$$S_0 = \sum_{n=1}^{N} \frac{a}{2} q^2_{n,t} + \frac{b}{2}\big(q_{n,t+1} + m^q_{n,t+1}\big)^2 + \mathcal{V}(q_{n,t}) - q_{n,t}\big(q_{n,t+1} + m^q_{n,t+1}\big) - m^p_{n,t+1} q_{n,t+1} \quad (4)$$

($a, b \in \mathbb{Z}$), and the second term, which cyclically couples neighboring particles, is

$$S_{\rm int} = -\sum_{n=1}^{N} q_{n,t}\, q_{1+(n \mod N),t}. \quad (5)$$

When the potential $\mathcal{V} = 0$, the map Φ_N is a linear automorphism, and we refer to it as a non-perturbed (otherwise perturbed) *coupled cat map* (CCM). From a general perspective, the map Φ_N is a particular example of coupled map lattices (CMLs), which are popular models for spatio-temporal chaos [20].

The equations of motion are generated by the function S (see Appendix). For our purposes, it is instructive to write them down in Newtonian form. Setting the n-th particle momentum to be $p_{n,t} = q_{n,t+1} - q_{n,t}$ from (14) and (15) given in Appendix A, we can write down

$$\Delta_t^2 q_{n,t} + \Delta_n^2 q_{n,t} = (a+b-4) q_{n,t} + \mathcal{V}'(q_{n,t}) \mod 1, \quad (6)$$

with the operator Δ^2_α standing for the discrete Laplacian $\Delta^2_\alpha f_\alpha \equiv f_{\alpha+1} - 2f_\alpha + f_{\alpha-1}$. At $\mathcal{V} = 0$, the action of Φ_N on vectors $\boldsymbol{q}_t$ and $\boldsymbol{p}_t$ is given by a band diagonal $2N \times 2N$ matrix $\mathcal{B}_N$, whose eigenvalues are the Lyapunov exponents λ_k of the system

$$\cosh(\lambda_k) = (a+b)/2 - \cos(2\pi k/N), \quad k = 1, \dots N. \quad (7)$$

The regime of fully chaotic dynamics is reached when $|\mathrm{Re}(\lambda_k)| > 0$ for all k, requiring that $|a+b| > 4$. In this case, it is quite easy to generate a PO for the system. Given an arbitrary set $\boldsymbol{\mathcal{M}}_0$ of $2N$ integers, the vector $((\mathcal{B}_N)^{\rm T} - 1)^{-1} \boldsymbol{\mathcal{M}}_0$ mod 1 provides initial conditions for the corresponding PO. The obtained data can then be used as a starting point to search for the PO of a perturbed map. When the perturbation $\mathcal{V}$ is not too strong, the system dynamics remain fully chaotic, and all POs are topologically conjugate to the unperturbed POs [14].

3. Spatio–temporal duality

Let us note here an important property of the model under consideration. The equation of motion (see (6)) possesses the symmetry under the exchange of time and particle numbers, $n \leftrightarrow t$. This immediately leads to the remarkable relation between POs of CCM — the so-called *spatio-temporal duality*. For each PO Γ of a period T of the N-particle map Φ_N, there exists a unique dual

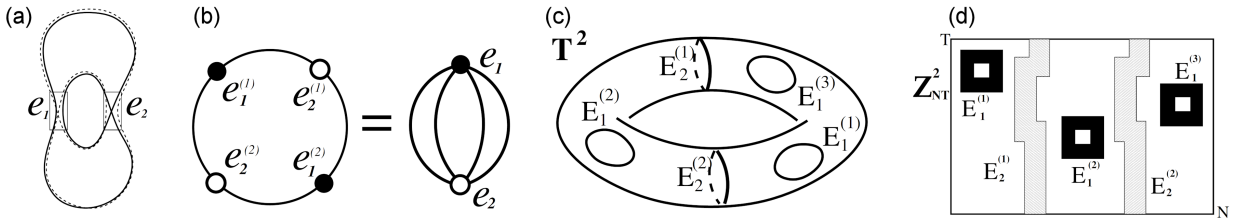

Fig. 1. Scheme of a pair of single-particle POs with two self-encounters, with the encounter regions marked by rectangles. (b) The left graph is the structural diagram of the PPO from panel (a); here, filled and empty circles correspond to encounters e_1 and e_2, respectively. The right graph ("Feynman diagram") was obtained after identification of the points belonging to the same encounters. (c) Structural χ diagram of many-particle PPO with one 2-encounter (E_2) of the type $w = (0, 1)$ and one 3-encounter (E_1) of the type $w = (0, 0)$. To obtain the "Feynman diagram," the black curves on the torus surface belonging to the same encounter have to be identified (glued up together). (d) Symbolic representation $\mathbb{M}_\Gamma$ of PO Γ with the encounter structure shown in panel (c). Two vertical (gray) and three (black) frame-like regions of $\mathbb{Z}^2_{\rm NT}$ mark the encounters, where Γ has identical symbolic representations.

T-particle PO Γ' of the map Φ_T with the period N. Furthermore, the actions and stabilities of both Γ and Γ' coincide. In particular, this implies that the number of N particle POs of the period T is the same as the number of T particle POs of the period N.

4. 2D-symbolic dynamics

To avoid this difficulty, we introduce a local 2D (rather than linear) symbolic dynamics with a small alphabet, allowing us to encode POs uniquely. Specifically, if Γ is a N-particle PO of a period T, we encode it with the toric $N \times T$ array of symbols $\mathbb{M}_\Gamma = \{\boldsymbol{m}_{n,t} | (n,t) \in \mathbb{Z}^2_{\rm NT}\}$, $\mathbb{Z}^2_{\rm NT} = [1 \dots N] \times [1 \dots T]$, where the integers $\boldsymbol{m}_{n,t} = (m^q_{n,t}, m^p_{n,t})$ are the corresponding local winding numbers of Γ. As only nearest neighbors are coupled in CCM, the size of such an alphabet does not depend on N. Given a 2D array $\mathbb{M}_\Gamma$, the corresponding PO can be uniquely restored (for $\mathcal{V} = 0$) by combining local winding numbers into global ones and then using them as an initial vector $\boldsymbol{\mathcal{M}}_0$ [16] (see Appendix B). The crucial property of the above symbolic dynamics is its locality. Namely, a fixed square of symbols $\{\boldsymbol{m}_{\bar{n},\bar{t}} | (\bar{n},\bar{t}) \in [n-r, \dots n+r] \times [t-r, \dots t+r]\}$ around a point (n,t) defines the position $q_{n,t}$ and the momentum $p_{n,t}$ of the n-th particle at time t up to an exponentially small error Λ^{-r}. Note that the symbolic dynamics possessing such properties are known to exist for certain CML [21].

5. Partner orbits correlation mechanism

Now we turn our attention to the correlation mechanism between POs. To explain our main idea and fix the notation, it is instructive to first consider a hypothetical continuous limit of the model where $n, t \in \mathbb{T}^2_{\rm NT} = [0, N] \times [0, T]$ instead of being integers. In this case, it is natural to think about a PO as a field $\Gamma(n,t) = (q_{n,t}, p_{n,t})$ (periodic in both n and t) which maps the n–t torus $\mathbb{T}^2_{\rm NT}$ upon a two-dimensional surface $\mathcal{S}^2_\Gamma$ in the q–p space. The above geometrical interpretation clearly indicates the essential differences in the correlation mechanism between many-particle and single-particle POs. Each l-encounter of a single-particle trajectory γ can be associated with a set of times $t_1, \dots t_l$ when γ approaches itself most closely. Thus, structurally different families of single-particle PPO can be distinguished by the order in which different encounters are attended (see Fig. 1b). On the other hand, a l-encounter of the field Γ is naturally associated with a set of identical (up to a shift) closed curves $\Upsilon^{(i)}$, $i = 1, \dots, l$ on $\mathbb{T}^2_{\rm NT}$ where the surface $\mathcal{S}^2_\Gamma$ approaches itself most faithfully in the q–p space, i.e., $\Gamma|_{\Upsilon^{(1)}} \approx \Gamma|_{\Upsilon^{(2)}} \cdots \approx \Gamma|_{\Upsilon^{(l)}}$ (see Fig. 1c). Each encounter, therefore, carries a pair of integers $\omega = (\omega^1, \omega^2)$ corresponding to the winding numbers of $\Upsilon^{(i)}$ along the n and t direction, respectively. Contrary to the single-particle dynamics, the structure of PPO is determined now by both the "topology" and the order of the encounters. In this case, structurally different families of PPOs can be classified with the help of 2D χ diagrams (see Fig. 1c).

Returning to the discrete case, we can utilize the 2D symbolic dynamics for a convenient description of the PO encounters structure. We say that a PO Γ possesses an l-encounter if there are l discrete identical (up to a shift) contours $\Upsilon^{(i)}$ on $\mathbb{Z}^2_{\rm NT}$ (i.e., $\Upsilon^{(i)} = \sigma^{(i)}(\Upsilon)$, $\sigma^{(i)}(n,t) \to (n + \Delta n_i \mod N, t + \Delta t_i \mod T)$ for some $(\Delta n_i, \Delta t_i)$, $i = 1, \dots l$ and Υ is a closed contour), such that the symbolic representation $\mathbb{M}_\Gamma$ is identical in the vicinity of each $\Upsilon^{(i)}$ (see Fig. 1d). In other words,

$$\mathbb{M}_\Gamma|_{\mathbb{E}^{(1)}} = \mathbb{M}_\Gamma|_{\mathbb{E}^{(2)}} \dots = \mathbb{M}_\Gamma|_{\mathbb{E}^{(l)}}, \qquad (8)$$

where $\mathbb{E}^{(i)} = \sigma^{(i)}(\mathbb{E})$ are the non-overlapping regions on $\mathbb{Z}^2_{\rm NT}$, which contain $\Upsilon^{(i)}$'s. Given that

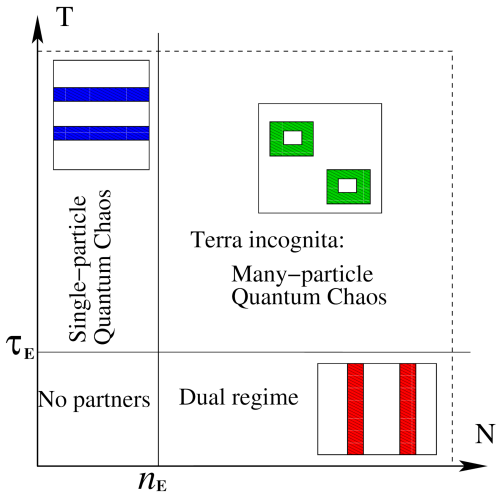

Fig. 2. Different regimes for semiclassical spectral correlations. In the few-particle regime, $T \gtrsim n_E \gtrsim N$, the dominant contribution to the off-diagonal part of the spectral form factor comes from the standard Sieber–Richter PPOs (and their multi-encounter extensions), which visit approximately the same points in the configuration space but in a different temporal order. In the dual short-time, many-body regime, $N \gtrsim n_E \gtrsim T$, the dominant contribution comes from PPOs that visit approximately the same points in the configuration space but in a different spatial order. In the most interesting case, where both time, T, and the number of particles, N, exceed the Ehrenfest scale n_E, the dominant contribution to spectral correlations arises from periodic orbits visiting approximately the same points in configuration space but in a different spatio–temporal order.

Γ possesses such an encounter, the locality of the symbolic dynamics guarantees that momenta and coordinates of the particles $\Gamma_{n,t} = (q_{n,t}, p_{n,t})$ at the encounter regions approach approximately the same values. The differences between $\Gamma_{n+\Delta n_i, t+\Delta t_i}$ and $\Gamma_{n+\Delta n_j, t+\Delta t_j}$ are decreasing exponentially with the "width" of the encounter regions $\mathbb{E}^{(i)}$. In the CCM model, the POs with a prescribed position and shape of the encounters Υ_i's can be found explicitly. The corresponding procedure is quite general and can be applied to an arbitrary encounter structure χ (see Appendix B). Having obtained such a trajectory Γ with encounters, it is straightforward to construct the partner PO $\bar{\Gamma}$ by reshuffling the symbolic representation $\mathbb{M}_\Gamma$ into one of its partners $\mathbb{M}_{\bar{\Gamma}}$. In the case of $\omega = (0,0)$ and $l = 2$, it is equivalent to the exchange of the symbolic representations in the interiors of $\Upsilon^{(1)}$ and $\Upsilon^{(2)}$ (see Fig. 2a). The resulting partners Γ and $\bar{\Gamma}$ approach approximately the same points of the q–p phase space, but in a different particle–time order. As in the single-particle case, the differences $\Delta S = S_\Gamma - S_{\bar{\Gamma}}$ between their actions are accumulated in the encounter regions, where the splittings between coordinates and the momenta become maximal (see Fig. 2b–d). Moreover, up to exponentially small corrections, the difference ΔS can be expressed as the sum along a contour Υ in the encounter region $\mathbb{E}$; this is written as $\sum_{(n,t)\in\Upsilon} \Delta S_{n,t}$, where $\Delta S_{n,t}$ is the local symplectic area of the parallelogram formed by four points $\Gamma_{n+\Delta n_1, t+\Delta t_1}$, $\Gamma_{n+\Delta n_2, t+\Delta t_2}$, $\bar{\Gamma}_{n+\Delta n_1, t+\Delta t_1}$, and $\bar{\Gamma}_{n+\Delta n_2, t+\Delta t_2}$ in the phase space [16]. This result naturally generalizes the analogous outcome for the action differences between the single-particle PPOs.

Summarizing, we emphasize that the PPO mechanism in a multiparticle system significantly expands due to the new type of encounters. The PPOs with the $\omega = (1,0)$ encounters reproduce the mechanism of correlations standard for the single-particle systems. At some instant of time, all N particles return to approximately the same positions they were in the past. On the other hand, PPO with the encounters of $\omega = (0,1)$ and $\omega = (0,0)$ types form completely new families. Indeed, these encounters involve only a small subset of particles (rather than all N) and cannot be interpreted as the single-particle encounters in the $2N$-dimensional phase space.

6. Spectral form factor

It is expected that the new classes of PPOs become essential for the semiclassical analysis of quantum systems with a sufficiently large number of particles. To test this, we consider a quantized CCM, whose time evolution is governed by an $L^N \times L^N$ unitary matrix U_N, with an integer L. The parameter L plays the role of the inverse Planck constant [13, 15].

Due to translational symmetry, the spectrum of U_N can be decomposed into N sectors, with approximately the same number of eigenvalues L^N/N. Most of them (except for either one or two sectors, see, e.g., [22]) come in pairs, leading to the double degeneracies in the system spectrum. The full spectral form-factor, including all symmetry components, is given by $K(N,T) = \langle |\mathrm{Tr}(U_N^T)|^2 \rangle / (2L^N)$, with the average taken over the ensemble generated by various perturbations $\mathcal{V}$[†]. Since the CCM exhibits chaotic dynamics, for a finite number of cat maps N and times T of the order of the Heisenberg time L^N/N (the standard "few-particle regime") we have

$$K(N,T) = K_\beta(N\,T/L^N), \tag{9}$$

where $K_\beta(\tau)$ is the universal spectral form-factor taken for the given symmetry class β of the model.

[†1] Here we assume that the map is generically perturbed. The spectra of non-peturbed cat maps are known to be of non-generic type because of large degeneracies among the periodic orbit actions (see [13]).

To address the case of large N, we make use of the spatio–temporal duality inherent to the model. The trace $\mathrm{Tr}(U_N^T)$, being written in the Gutzwiller trace-like form, is expressed through the sum over periodic orbits (POs) of the period T (see Appendix C). Furthermore, for coupled cat map (CCM), this representation is exact [15, 19]. Since POs of the classical map Φ_N with the period T are conjugated to POs of the map Φ_T with the period N, i.e., they possess the same actions and stabilities, we arrive at the relation

$$\mathrm{Tr}\Big((U_N)^T \Big) = \mathrm{Tr}\Big((U_T)^N \Big). \tag{10}$$

Here, the $L^T \times L^T$ unitary matrix U_T plays the role of spatial evolution and has exactly the same form as the temporal evolution operator for the CCM chain of length T. The relation (10) is the quantum counterpart of the classical spatio–temporal duality of CCM. It is reminiscent of the Nelson symmetry known to exist in the Euclidean field theories [23]. It is worth noting that the CCM belongs to the class of *dual-unitary* models, in which both spatial and temporal evolutions are governed by unitary operators. For the CCM, these two evolutions essentially coincide. In recent years, the dual-unitary models have attracted considerable attention [24–38] due to their intriguing properties. On the one hand, such systems demonstrate quantum properties akin to those of maximally chaotic many-body systems, such as Wigner–Dyson spectral statistics and insusceptibility to many-body localization effects [39–41]. On the other hand, the dual-unitary models are amenable to exact treatment. In particular, due to the combination of duality and causality, the local two-point correlation functions in these systems can be calculated exactly [27, 42–44].

From (10), it immediately follows that the regime of finite times T and a large number of particles $NT \sim L^T$ can be related to the universal regime (i.e., provided by RMT), where N is finite and $NT \sim L^N$. Specifically, for $NT \sim L^T$, the duality relation (10) yields

$$K(N,T) = L^{T-N}\, K_\beta(NT/L^T), \tag{11}$$

where it is assumed that different subspectra of U_T are uncorrelated and belong to the same universality class β. Particularly, for very short times $L^T/T \lesssim N$, one has $K_\beta \approx 1$, and we find the exponential growth of the form factor with T as $K(N,T) \approx L^{T-N}$. For somewhat larger (but finite) times, $L^T/T \gtrsim N$, one gets $K_\beta(\tau) \approx 2\tau/\beta + \mathcal{O}(\tau^2)$, which, to the leading order, yields the expected linear in-time growth of the form factor, i.e., $K(N,T) \approx 2NT/(\beta L^N)$.

Written in semiclassical form, the form factor $K(N,T)$ splits into the diagonal and off-diagonal contributions,

$$\left(\frac{L^N}{NT}\right) K(N,T) = \mathcal{K}_{\mathrm{diag}}(N,T) + \sum_\chi \mathcal{K}_{\mathrm{off}}^{(\chi)}(N,T). \tag{12}$$

The first term can be evaluated in a standard way, leading to $\mathcal{K}_{\mathrm{diag}}(N,T) = 2/\beta$ regardless of the regime considered, i.e., the relation between N and T. The second term accounts for correlations between PPOs with various χ structures. Which of the χ structures is responsible for the essential contribution depends crucially on N and T. To distinguish between the different regimes, we introduce an Ehrenfest-like parameter $n_E = \lambda_{\min}^{-1} \log(L)$ with $\lambda_{\min}$ being the lowest Lyapunov exponent of the system, given for the CCM by $\cosh(\lambda_{\min}) = (a+b-2)/2$, as follows from (7). Note that the spatio–temporal duality of our model implies equality between n_E and the Ehrenfest time τ_E.

For $N \lesssim n_E \lesssim T$, the essential contribution to $K(N,T)$ is provided by $\omega = (1,0)$ PPOs. Indeed, to reach the scale L^{-1} between the action difference of the PPOs, the width of the encounters has to be of the order of n_E. This is effectively the "single-particle" regime, and the PPO correlations lead to the universal result. In the dual regime $T \lesssim n_E \lesssim N$, the essential contribution to $K(N,T)$ arises from the $\omega = (0,1)$ PPOs, whose actions and stabilities mirror the ones of the "single-particle" PPOs with the encounters of $\omega = (1,0)$ type (see Fig. 2).

Finally, we give a rough estimation of $\mathcal{K}_{\mathrm{off}}^{(\chi)}$ in the "many-particle" regime $N, T \gtrsim n_E$. As in the single-particle case, the contribution from a family of PPOs includes two factors. The first one arrives from the probability of a given encounter structure realization, while the second one is due to the action differences. Combined, they yield contributions proportional to $(TN)^k/L^l$, where k is the number of encounters and l is the total length of the encounters (i.e., the number of points on the discretized contours Υ_i). For encounters winding around the torus in the particle (respectively, time) direction, we estimate $l = Nk$ (or equivalently, $l = Tk$), while for the $\omega = (0,0)$ encounters, the relevant length scale of Υ_i is provided by n_E, yielding $l \sim k n_E$. The expected contribution from PPO is therefore written as

$$\mathcal{K}_{\mathrm{off}}^{(\chi)}(N,T) = \sum_{k=1}^{\infty} \alpha_\chi^{(k)} \left(\frac{NT}{L^{d_\omega}}\right)^k, \tag{13}$$

where $d_{(1,0)} = N$, and $d_{(0,1)} = T$, while $d_{(0,0)} \sim n_E$ for the $\omega = (0,0)$ type of encounters. Although presently the coefficients $\alpha_\chi^{(k)}$ are known explicitly only for the standard $\omega = (1,0)$ PPO types (and, by the duality relation, also for $\omega = (0,1)$ PPO), the generic form of (13) indicates that in the $N, T \gtrsim n_E$ regime the dominant contribution is supplied by the $\omega = (0,0)$ PPOs. We remind the reader that the semiclassical expansion of (13) is expected to be valid only up to the respective "Heisenberg" time $NT < L^{d_\omega}$. Beyond these scales, the PO pairing mechanism changes its nature [45, 46], leading, for instance, to a non-analytic behavior of the form factor.

7. Conclusions

The semiclassical theory of chaotic systems rests upon the existence of partner periodic orbits (PPOs) with small action differences. For systems composed of only a few particles, these orbits begin contribute to spectral correlations when their periods exceed the Ehrenfest time τ_E, leading to universal RMT results on the time scales $T \sim T_H$. As we demonstrate in this work, the established picture must be fundamentally revised for chaotic systems composed of a large number (N) of particles. Using the coupled cat maps model, we show that in chaotic systems with local homogeneous interactions, a scale n_E, analogous to τ_E, emerges for the particle number. For the regime $N \lesssim n_E$, the standard correlation mechanism between periodic orbits prevails. However, once $N \gtrsim n_E$, the situation changes. In the short-time thermodynamic regime, when $T \lesssim n_E \lesssim N$, the correlation mechanism between periodic orbits becomes dual to the standard one observed in few-body systems. In particular, at very short times, this dual mechanism leads to an exponential growth of the spectral form factor with T. Finally, in the most challenging case, where both N and T exceed the Ehrenfest scale n_E (respectively, τ_E), a new type of correlation between periodic orbits emerges. These spatio–temporal correlations are specific to many-particle systems and become dominant over the standard Sieber–Richter type of correlations [6], as illustrated in Fig. 2.

Acknowledgments

We are indebted to M. Akila, T. Guhr, D. Waltner, and the late P. Braun for valuable discussions. The support of the Israel Science Foundation through Grant No. 2089/19 is gratefully acknowledged.

Appendix

A. Dynamical equations for CCM

The equations of motion for CCM are determined by $p_{n,t} = -\partial S/\partial q_{n,t}$, $p_{n,t+1} = \partial S/\partial q_{n,t+1}$, where the interacting and non-interacting parts of the generating function S are given by (4) and (5). This yields

$$q_{n,t+1} = p_{n,t} + a\, q_{n,t} - q_{n+1,t} + q_{n-1,t} - m^q_{n,t+1} + \mathcal{V}'(q_{n,t}), \tag{14}$$

$$p_{n,t+1} = (-p_{n,t} - (1-a\,b)q_{n,t}) - b\,(q_{n+1,t} + q_{n-1,t}) - m^p_{n,t+1} - \mathcal{V}'(q_{n,t}). \tag{15}$$

Under the condition $\mathcal{V}(q) \equiv 0$, these equations can be recast in the matrix representation

$$\begin{aligned} &Z_{t+1} = \mathcal{B}_N Z_t \mod 1, \\ &Z_t = (q_{1,t}, p_{1,t}, \dots q_{N,t}, p_{N,t})^{\mathrm{T}}, \end{aligned} \tag{16}$$

with a $2N \times 2N$ matrix $\mathcal{B}_N$ given by

$$\mathcal{B}_N = \begin{pmatrix} A & B & \mathbf{0} & \dots & \mathbf{0} & B \\ B & A & B & \dots & \mathbf{0} & \mathbf{0} \\ \mathbf{0} & B & A & \dots & \mathbf{0} & \mathbf{0} \\ \vdots & \vdots & \vdots & \ddots & \vdots & \vdots \\ \mathbf{0} & \mathbf{0} & \mathbf{0} & \dots & A & B \\ B & \mathbf{0} & \mathbf{0} & \dots & B & A \end{pmatrix}, \tag{17}$$

where

$$A = \begin{pmatrix} a & 1 \\ ab-1 & b \end{pmatrix}, \qquad B = -\begin{pmatrix} 1 & 0 \\ b & 0 \end{pmatrix}. \tag{18}$$

B. Construction of many-particle PPO for $\mathcal{V} = 0$

The construction of PPOs with the prescribed encounter structure can be done in four steps, described below. We illustrate this procedure using a particular example of partner POs possessing the encounter of $\omega = (0, 0)$ type (see Fig. 3).

Step 1. As the first step, we generate a random PO and its symbolic representation. To this end, we take $\boldsymbol{\mathcal{M}}_0$ to be an arbitrary vector of integers. Then the $2N$-dimensional vector

$$\begin{aligned} &\boldsymbol{Z}_0 = (\mathcal{B}_N^T - I)^{-1}\boldsymbol{\mathcal{M}}_0 \mod \mathbf{1}, \\ &\boldsymbol{Z}_0 = (\boldsymbol{q}^{(0)}, \boldsymbol{p}^{(0)})^{\mathrm{T}}, \end{aligned} \tag{19}$$

defines the initial coordinates $\boldsymbol{q}^{(0)}$ and momenta $\boldsymbol{p}^{(0)}$ of some PO Γ_0. The whole range of Γ_0 data can be restored from the iterative action of the matrix $\mathcal{B}_N$ on the vector $\boldsymbol{Z}_0$. Since the entries of the matrix $\mathcal{B}_N$ are integers, the coordinates and momenta of Γ_0 are rational numbers. This allows us to calculate POs explicitly, avoiding any numerical approximations.

Step 2. For small N and T, the PO Γ_0 generically does not have any encounters, so the purpose of this step is to prepare an orbit with encounters. To do this, we choose some region $\mathbb{E} \subset \mathbb{Z}^2_{\mathrm{NT}}$ of some given shape (annular-like, as in the example in Fig. 3). Next, the symbols $\mathbb{M}_{\Gamma_0}|_{\mathbb{E}}$ are copied and pasted upon another region $\mathbb{E}'$, which is obtained by a shift of $\mathbb{E}$ such that $\mathbb{E} \cap \mathbb{E}' = \emptyset$. The resulting sequence of symbols $\widetilde{\mathbb{M}}_{\Gamma_0}$ has the required encounter structure, but, in general, does not correspond to any real PO.

Step 3. To generate a 2D sequence of symbols corresponding to a valid periodic orbit, we use the sequence $\widetilde{\mathbb{M}}_{\Gamma_0}$ as it would be a real set of local winding numbers. More specifically, let $\widetilde{\boldsymbol{M}}_t := \widetilde{\mathbb{M}}_{\Gamma_0}(t)$ be the t-th column of $\widetilde{\mathbb{M}}_{\Gamma_0}$. We define the integer vector of global "winding numbers" as

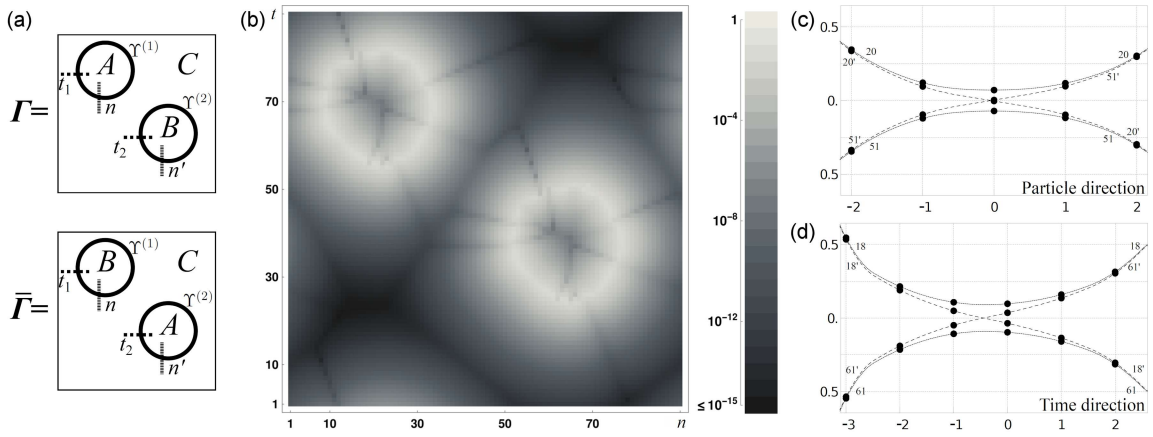

Fig. 3. (a) Diagrams of two partner periodic orbits with the annular encounters, $w = (0, 0)$. The identical fields A, B, C are separated by the encounter line ℓ. The dashed lines depict the sections of ℓ for the plots c and d. (b) Logarithm of the metric distances (see (4)) between the paired points of PPO for the map (see (19)) with the parameters $a = 3$, $b = 2$, $r = 1$, $T = N = 90$; the maximal distance is $\sim 1.5 \times 10^{-3}$. (c) Relative coordinates (see explanations in the text) of 5 neighboring particles taken in the encounter region, in this realization, the particles 7–11 are taken at time $t_1 = 70$, and particles 50–54 at $t_2 = 39$. (d) Dynamics of the particle relative coordinates in the encounter region, $m = 18$ and $m' = 61$ at times 53–58 and 22–27, respectively.

$$\widetilde{\mathcal{M}}_0 = \sum_{t=1}^{T} \mathcal{B}_N^{T-t} \widetilde{M}_t. \tag{20}$$

It is then used as an input for the right-hand side of (19). The resulting PO, denoted as Γ, has the 2D symbolic representation $\mathbb{M}_\Gamma$. The crucial observation is that $\mathbb{M}_\Gamma$ and $\widetilde{\mathbb{M}}_{\Gamma_0}$ differ only locally at the places of the encounter boundaries. As a result, we obtain the PO Γ with the desired encounter structure.

Step 4. At this stage, we can construct the partner orbit $\bar{\Gamma}$ by rearranging the symbols $\mathbb{M}_\Gamma$ outside of the encounter regions into a new 2D sequence $\mathbb{M}_{\bar{\Gamma}}$. For the example in Fig. 3, it amounts to the exchange of symbols at the regions A and B, i.e.,

$$\mathbb{M}_{\bar{\Gamma}}|_A = \mathbb{M}_\Gamma|_B, \quad \mathbb{M}_{\bar{\Gamma}}|_B = \mathbb{M}_\Gamma|_A, \quad \mathbb{M}_{\bar{\Gamma}}|_C = \mathbb{M}_\Gamma|_C. \tag{21}$$

Note that this new sequence of symbols is, in fact, a symbolic representation of a valid PO $\bar{\Gamma}$, which can be straightforwardly recovered from $\mathbb{M}_{\bar{\Gamma}}$.

As an example, we generated a PPO with annular encounters by following the above 4-step protocol. By construction $\bar{\Gamma}$ and Γ, are PPO traversing approximately the same points of the phase space but in different n–t order, i.e., $\bar{\Gamma}_{n',t'} \approx \Gamma_{n,t}$, where $(n', t') = P(n, t)$ are given by a certain permutation P of indexes (n, t). The metric distances

$$d(n,t) = \sqrt{(q_{n,t} - \bar{q}_{n',t'})^2 + (p_{n,t} - \bar{p}_{n',t'})^2} \tag{22}$$

between the paired points of Γ and $\bar{\Gamma}$ are plotted in Fig. 3b. As expected, the largest distances between the orbits are reached in the encounter region, and the orbits' deviations from each other decrease exponentially fast in the perpendicular directions to the encounter contour. In Fig. 3d, we demonstrate the encounter portraits in two sections, cutting the encounter line ℓ along the particle (p.w.) and time (t.w.) directions (see the dashed lines in Fig. 3a).

C. Gutzwiller trace formula for CCM

Quantization of general multidimensional cat maps was studied in [15], where the following trace formula was derived

$$\mathrm{Tr}\,(U_N)^T = \left|\det(\mathcal{B}_N^T - 1)\right|^{-\frac{1}{2}} \sum_{\Gamma \in \mathrm{PO}} \exp(-\mathrm{i}2\pi L S_\Gamma). \tag{23}$$

Here, S_Γ is the classical action of PO Γ, and the sum runs over all POs of the period T. Note that the square of the prefactor in front of the sum determines the total number of POs with the period T and is symmetric under the exchange $N \leftrightarrow T$. The above equation is a precise analog of (1), which for non-perturbed CCM is exact, instead of being a semiclassical approximation.

References

[1] M.C. Gutzwiller, *J. Math. Phys.* **12**, 343 (1971).

[2] F. Haake, *Quantum Signatures of Chaos*, 3d ed., Springer, Heidelberg 2010.

[3] M. Berry, *Proc. R. Soc. Lond. A* **400**, 229 (1985).

[4] O. Bohigas, M.J. Giannoni, C. Schmit, *Phys. Rev. Lett.* **52**, 1 (1984).

[5] G. Casati, I. Guarneri, F. Valz-Gris, *Lett. Nuovo Cimento* **28**, 279 (1980).

[6] M. Sieber, K. Richter, *Phys. Scr.* **2001**, 128 (2001).

[7] M. Sieber, *J. Phys. A* **35**, L613 (2002).

[8] S. Müller, S. Heusler, P. Braun, F. Haake, A. Altland, *Phys. Rev. Lett.* **93**, 014103 (2004).

[9] S. Müller, S. Heusler, P. Braun, F. Haake, A. Altland, *Phys. Rev. E* **72**, 046207 (2005).

[10] T. Engl, J. Dujardin, A. Argüelles, P. Schlagheck, K. Richter, J.D. Urbina, *Phys. Rev. Lett.* **112**, 140403 (2014).

[11] J.H. Hannay, M.V. Berry, *Physica D* **1**, 267 (1980).

[12] J.P. Keating, *Nonlinearity* **4**, 277 (1991).

[13] J.P. Keating, *Nonlinearity* **4**, 309 (1991).

[14] P.A. Boasman, J.P. Keating, *Proc. R. Soc. Lond. A* **449**, 629 (1995).

[15] A.M.F. Rivas, M. Saraceno, A.M.O. de Almeida, *Nonlinearity* **13**, 341 (2000).

[16] B. Gutkin, V.Al. Osipov, *Nonlinearity* **29**, 325 (2016).

[17] B. Gutkin, P. Cvitanović, R. Jafari, A.K. Saremi, L. Han, *Nonlinearity* **34**, 2800 (2021).

[18] H. Liang, P. Cvitanović, *J. Phys. A Math. Theor.* **55**, 304002, (2022).

[19] I. Fouxon, B. Gutkin, *J. Phys. A Math. Theor.* **55**, 504004, (2022).

[20] K. Kaneko, in: *Formation, Dynamics, and Statistics of Patterns*, Eds. K. Kawasaki, M. Suzuki, World Scientific, Singapore 1990, p. 1.

[21] S.D. Pethel, N.J. Corron, E. Bollt, *Phys. Rev. Lett.* **99**, 214101 (2007).

[22] C. Pineda, T. Prosen, *Phys. Rev. E* **67**, 061127 (2007).

[23] E. Nelson, *J. Funct. Anal.* **12**, 97 (1973).

[24] M. Akila, D. Waltner, B. Gutkin, T. Guhr, *J. Phys. A Math,. Theor.* **49**, 375101 (2016).

[25] B. Bertini, P. Kos, T. Prosen, *Phys. Rev. Lett.* **121**, 264101 (2018).

[26] B. Bertini, P. Kos, T. Prosen, *Phys. Rev. X* **9**, 021033 (2019).

[27] B. Bertini, P. Kos, T. Prosen, *Phys. Rev. Lett.* **123**, 210601 (2019).

[28] S.A. Rather, S. Aravinda, A. Lakshminarayan, *Phys. Rev. Lett.* **125**, 070501 (2020).

[29] S. Gopalakrishnan, A. Lamacraft, *Phys. Rev. B* **100**, 064309 (2019).

[30] R. Pal, A. Lakshminarayan, *Phys. Rev. B* **98**, 174304 (2018).

[31] P. Braun, D. Waltner, M. Akila, B. Gutkin, T. Guhr, *Phys. Rev. E* **101**, 052201 (2020).

[32] L. Piroli, B. Bertini, J.I. Cirac, T. Prosen, *Phys. Rev. B* **101**, 094304 (2020).

[33] B. Bertini, P. Kos, T. Prosen, *SciPost Phys.* **8**, 067 (2020).

[34] P. Kos, B. Bertini, T. Prosen, *Phys. Rev. X* **11**, 011022 (2021).

[35] T. Zhou, A. Nahum, *Phys. Rev. X* **10**, 031066 (2020).

[36] J. Avan, V. Caudrelier, A. Doikou, A. Kundu, *Nucl. Phys. B* **902**, 415 (2016).

[37] D. Goyeneche, D. Alsina, J.I. Latorre, A. Riera, K. Życzkowski, *Phys. Rev. A* **92**, 032316 (2015).

[38] S. Aravinda, S.A. Rather, A. Lakshminarayan, *Phys. Rev. Res.* **3**, 043034 (2021).

[39] B. Bertini, P. Kos, T. Prosen, *Phys. Rev. Lett.* **121**, 264101 (2018).

[40] P. Braun, D. Waltner, M. Akila, B. Gutkin, T. Guhr, *Phys. Rev. E* **101**, 052201 (2020).

[41] A. Chan, A. De Luca, J.T. Chalker, *Phys. Rev. Res.* **3**, 023118 (2021).

[42] B. Gutkin, P. Braun, M. Akila, D. Waltner, T. Guhr, *Phys. Rev. B* **102**, 174307 (2020).

[43] P.W. Claeys, A. Lamacraft, "Maximum velocity quantum circuits", *Phys. Rev. Res.* **2**, 033032 (2020).

[44] V. Al. Osipov, N. Krieger, T. Guhr, B. Gutkin, *Phys. Rev. B* **109**, 214302 (2024).

[45] B. Gutkin, V.Al. Osipov, *Nonlinearity* **26**, 177 (2013).

[46] B. Gutkin, V.Al. Osipov, *J. Stat. Phys.* **153**, 1049 (2013).